LETTER

doi:10.1038/nature11468

Increased proteasome activity in human embryonic stem cells is regulated by PSMD11

David Vilchez[1], Leah Boyer[2], Ianessa Morantte[1], Margaret Lutz[3], Carsten Merkwirth[1], Derek Joyce[1], Brian Spencer[4], Lesley Page[5], Eliezer Masliah[4], W. Travis Berggren[3], Fred H. Gage[2] & Andrew Dillin[1]

Embryonic stem cells can replicate continuously in the absence of senescence and, therefore, are immortal in culture[1,2]. Although genome stability is essential for the survival of stem cells, proteome stability may have an equally important role in stem-cell identity and function. Furthermore, with the asymmetric divisions invoked by stem cells, the passage of damaged proteins to daughter cells could potentially destroy the resulting lineage of cells. Therefore, a firm understanding of how stem cells maintain their proteome is of central importance. Here we show that human embryonic stem cells (hESCs) exhibit high proteasome activity that is correlated with increased levels of the 19S proteasome subunit PSMD11 (known as RPN-6 in *Caenorhabditis elegans*)[3–5] and a corresponding increased assembly of the 26S/30S proteasome. Ectopic expression of PSMD11 is sufficient to increase proteasome assembly and activity. FOXO4, an insulin/insulin-like growth factor-I (IGF-I) responsive transcription factor associated with long lifespan in invertebrates[6,7], regulates proteasome activity by modulating the expression of PSMD11 in hESCs. Proteasome inhibition in hESCs affects the expression of pluripotency markers and the levels of specific markers of the distinct germ layers. Our results suggest a new regulation of proteostasis in hESCs that links longevity and stress resistance in invertebrates to hESC function and identity.

Embryonic stem cells are unique among all stem-cell populations examined in that they do not seem to undergo replicative senescence[1,2]. Because proteostasis is crucial for maintaining proper cell function[8,9], hESCs could provide a new model to define proteostasis regulation and its demise in ageing. Central to proteostasis is the ubiquitin proteasome system and we examined whether proteasome activity changes as hESCs differentiate into several cell lineages. To evaluate differences in the 26S/30S proteasome activity, we monitored the degradation of specific fluorogenic peptide substrates[10]. We differentiated H9 hESCs into neural progenitors cells (NPCs) and observed a marked decrease in the chymotrypsin-like proteasome activity (Fig. 1a). Moreover, when NPCs were differentiated into neurons, we detected a further decrease in proteasome activity during the differentiation process that was observable after 2 weeks (Fig. 1a and Supplementary Fig. 1). Consistent with enhanced proteasome activity in hESCs, we found increased levels of polyubiquitinated proteins in differentiated cells compared with hESCs (Fig. 1b). Because hESCs are known to vary in their characteristics despite unlimited capacity of self-renewal[11], we differentiated a distinct hESC line, HUES-6 cells, and obtained similar results (Supplementary Figs 1 and 2). Proteasome inhibitors blocked activity from extracts of hESCs, NPCs and neurons (Supplementary Fig. 3), indicating that the increased peptidase activity was indeed due to the proteasome. In addition, the other two activities of the proteasome, the caspase-like and trypsin-like activities, were also increased in hESCs (Supplementary Fig. 4). Proteasome activity did not differ depending on the passage number (Supplementary Fig. 5). The decrease in proteasome activity was not a specific phenomenon associated with the neural lineage as differentiation into either trophoblasts or fibroblasts induced a similar decrease (Fig. 1c, d).

Notably, hESCs lost their high proteasome activity in a continuous progressive manner during the differentiation process (Fig. 1c). Moreover, we examined other cell lines extracted from human tissues, such as astrocytes, BJ fibroblasts or immortalized HEK293T cells, and found that these cells also had lower proteasome activity compared with hESCs (Supplementary Fig. 6). We tested whether high proteasome activity in hESCs was associated with increased proliferation and found

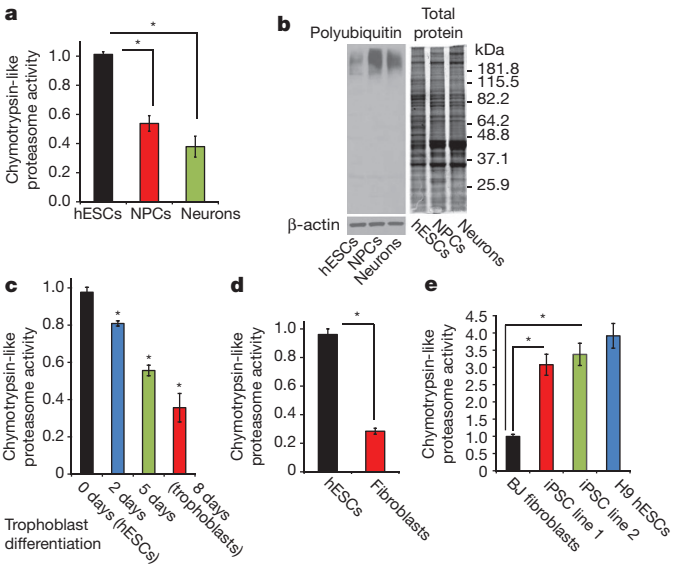

Figure 1 | Increased proteasome activity in hESCs. **a**, Chymotrypsin-like (Z-Gly-Gly-Leu-AMC) proteasome activity (relative slope to H9 hESCs) is shown. hESCs ($n = 11$), NPCs ($n = 13$), neurons ($n = 10$); $^*P < 0.00001$. **b**, Representative immunoblot of polyubiquitinated protein levels. β-actin is the loading control. Total protein was visualized by Coomassie staining. **c**, Chymotrypsin-like proteasome activity (relative slope to H9 hESCs) is shown. hESCs ($n = 6$), 2 days of differentiation into trophoblasts ($n = 6$), 5 days ($n = 6$), 8 days ($n = 7$). hESCs versus 2 days, $^*P < 0.001$; hESCs versus 5 days, $^*P = 7.7 \times 10^{-7}$; hESCs versus 8 days, $^*P < 0.0001$. **d**, Chymotrypsin-like proteasome activity (relative slope to H9 hESCs) is shown. hESCs ($n = 3$), fibroblasts ($n = 3$); $^*P < 0.001$. **e**, Chymotrypsin-like proteasome activity (relative slope to BJ fibroblasts) is shown. BJ fibroblasts ($n = 10$), iPSC line 1 ($n = 10$), iPSC line 2 ($n = 9$), H9 hESCs ($n = 5$). iPSC lines have increased proteasome activity compared with fibroblasts ($^*P < 0.0005$), and no significant differences compared with H9 hESCs (iPSC line 1 versus hESCs, $P = 0.11$; iPSC line 2 versus hESCs, $P = 0.29$). In **a**, **c**, **d** and **e** data represent the mean ± s.e.m. All statistical comparisons were made by Student's *t*-test for unpaired samples.

[1]Howard Hughes Medical Institute, Glenn Center for Aging Research, Molecular and Cell Biology Laboratory, The Salk Institute for Biological Studies, 10010 North Torrey Pines Road, La Jolla, California 92037, USA. [2]Laboratory of Genetics, The Salk Institute for Biological Studies, 10010 North Torrey Pines Road, La Jolla, California 92037, USA. [3]Stem Cell Core, The Salk Institute for Biological Studies, 10010 North Torrey Pines Road, La Jolla, California 92037, USA. [4]Department of Neurosciences, University of California, San Diego, 9500 Gilman Drive, La Jolla, California 92093, USA. [5]Department of Cell Biology, The Scripps Research Institute, 10550 North Torrey Pines Road, La Jolla, California 92037, USA.

that hESCs and HEK293T cells had nearly identical proliferation rates, yet hESCs had higher proteasome activity (Supplementary Fig. 7). Induced pluripotent stem cells (iPSCs) can be derived from adult somatic cells by forced expression of exogenous factors that promote cell reprogramming[12–14]. iPSC lines are similar to embryonic stem cells in many respects, such as their gene expression patterns, proteome profile and potential for differentiation[13,15]. However, the full extent of their similarity to embryonic stem cells is still being assessed[16]. We analysed two iPSC lines that had been carefully validated to ensure similar gene expression profiles, growth characteristics and developmental potentials to hESCs[17]. We discovered that these iPSC lines derived from BJ fibroblasts display increased proteasome activity similar to hESCs (Fig. 1e), indicating that proteasomal activity can indeed be reprogrammed.

The 26S/30S proteasome consists of a 20S core structure containing the proteolytic active sites and 19S cap structures that impart regulation on the activity of the holo-complex (26S, single and 30S, double capped)[18]. Although 20S particles can exist in a free form, 20S particles

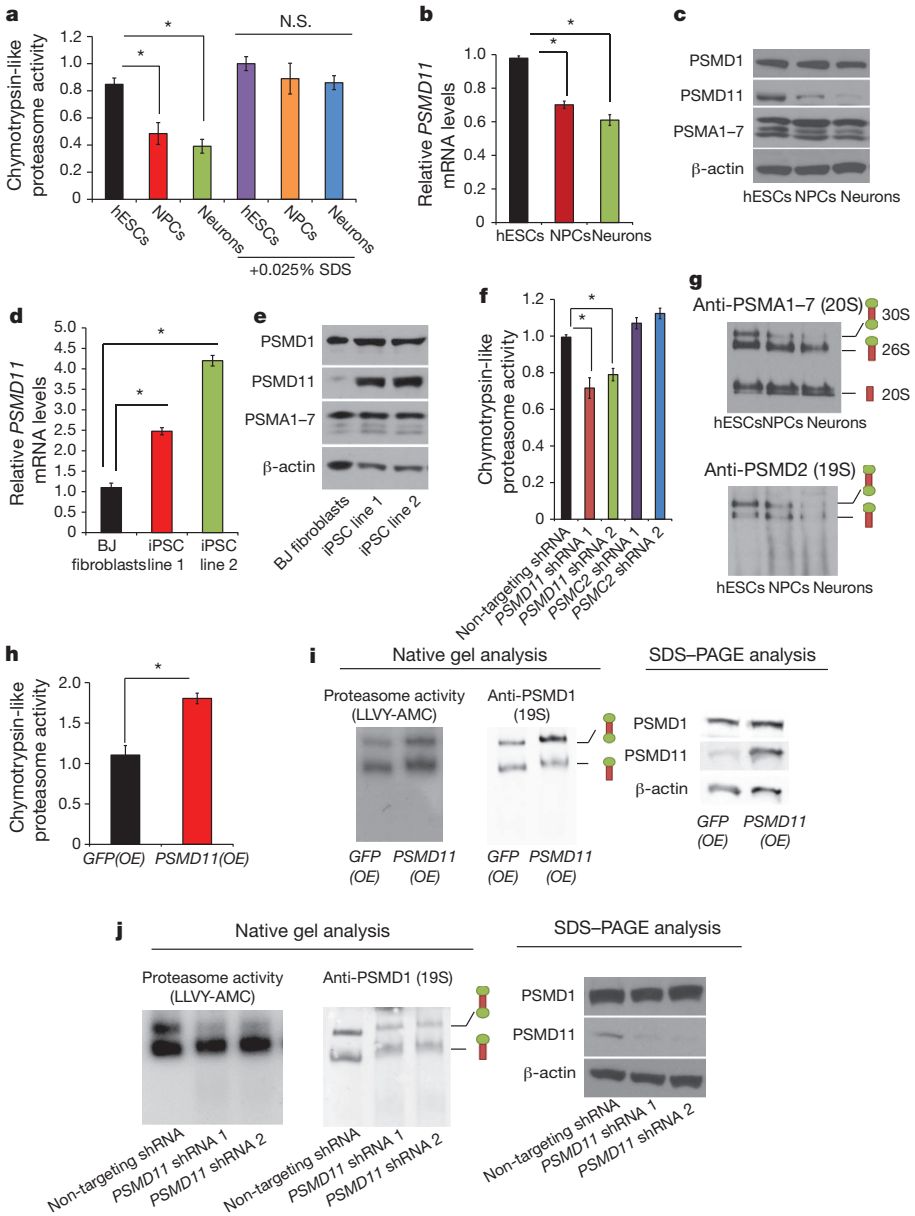

Figure 2 | Increased proteasome assembly in hESCs depends on PSMD11 expression. **a**, Chymotrypsin-like proteasome activity (relative slope to H9 hESCs + 0.025% SDS) is shown. $n = 4–6$; $^*P < 0.01$. No significant differences (N.S.) were found among the different cells when SDS was added (hESCs + SDS versus NPCs + SDS, $P = 0.25$; hESCs + SDS versus neurons + SDS, $P = 0.09$). **b**, Relative *PSMD11* expression compared with H9 hESCs. hESCs ($n = 10$), NPCs ($n = 6$), neurons ($n = 8$); $^*P < 0.00001$. **c**, **e**, Western blot analysis with antibodies against PSMA1–7, PSMD11 and PSMD1. β-actin is the loading control. **d**, Relative *PSMD11* expression compared with BJ fibroblasts. BJ fibroblasts ($n = 10$), iPSC line 1 ($n = 6$), iPSC line 2 ($n = 6$); $^*P < 0.00001$. **f**, Proteasome activity (relative slope to lentivirus non-targeting shRNA) is shown. Non-targeting shRNA ($n = 10$), *PSMD11* shRNA 1 ($n = 8$), *PSMD11* shRNA 2 ($n = 6$), *PSMC2* shRNA 1 ($n = 6$), *PSMC2* shRNA 2 ($n = 3$); $^*P < 0.01$. **g**, Native gel electrophoresis followed by western blot with PSMA1–7 (20S subunit) or PSMD2 (19S subunit) antibodies. **h**, Chymotrypsin-like proteasome activity (relative slope to green fluorescent protein (GFP) overexpressing (OE) HEK293T cells) is shown. *GFP(OE)* ($n = 4$), *PSMD11(OE)* ($n = 5$); $^*P < 0.005$. **i**, **j**, Native gel electrophoresis of HEK293T cell extracts followed by proteasome activity assay with chymotrypsin-like activity substrate Leu-Leu-Val-Tyr-AMC and immunoblotting with PSMD1 (19S subunit) antibody are shown. Extracts were resolved by SDS–PAGE and immunoblotting for analysis of PSMD11 levels and β-actin loading control. In **a**, **b**, **d**, **f** and **h**, data represent the mean ± s.e.m. All statistical comparisons were made by Student's *t*-test for unpaired samples.

in their most physiological form are inactive, unable to degrade denatured proteins or cleave peptides[10]. The 19S regulatory subunit is responsible for stimulating the 20S proteasome to degrade proteins, because ATPases of the regulatory particle open the 20S core, allowing substrates access to proteolytic active sites[19]. SDS treatment of cell extracts, a condition that activates 20S particles by allowing gate opening[20], resulted in equivalent activities among all cell types (Fig. 2a and Supplementary Fig. 8). This result suggests that all cell types have an equal number of 20S particles, but hESCs have increased levels of active 26S/30S proteasomes. We examined the expression of the different 19S proteasome subunits and observed that PSMD11 was the only 19S subunit to decrease as hESCs differentiated (Fig. 2b, c and Supplementary Figs 9–12). Consistent with the hESCs results, we observed increased PSMD11 levels in iPSCs (Fig. 2d, e). Accordingly, decreased expression of PSMD11 in hESCs (Supplementary Table 1) reduced proteasome activity (Fig. 2f), demonstrating that the increased levels of this subunit in hESCs are crucial for increased proteasome activity. PSMD11 has a vital role in stabilizing the otherwise weak interaction between the 20S core and the 19S cap[4], suggesting that hESCs might have more assembled proteasomes. We detected more 30S particles in hESCs compared with NPCs and neurons. Furthermore, as more 20S subunits are assembled into 30S particles, less free 20S is found in hESCs (Fig. 2g). Ectopic expression of PSMD11 was sufficient to increase proteasome activity and assembly in cells with relatively low proteasome activity (Fig. 2h, i). Moreover, knockdown of PSMD11 resulted in fewer assembled proteasomes (Fig. 2j).

The levels of RPN-6, the *C. elegans* orthologue of PSMD11, are increased in the long-lived *glp-1* mutant. In this mutant, increased proteasome activity, *rpn-6* expression and longevity are modulated by the forkhead box O (FOXO) transcription factor DAF-16. To examine whether FOXO transcription factors regulate proteasome activity in hESCs, we reduced expression of the closest human *daf-16* orthologues FOXO1, FOXO3 and FOXO4 (Supplementary Fig. 13 and Supplementary Table 2). Notably, we found that FOXO4 was crucial to modulate proteasome activity in hESCs, whereas FOXO1 and FOXO3, as well as a HSF1, had little or no effect on proteasome activity (Fig. 3a, b and Supplementary Fig. 14). As hESCs differentiated into neural cells, trophoblasts or fibroblasts, there was a corresponding decrease in FOXO4 expression (Supplementary Figs 15–17). Accordingly, this decrease in FOXO4 expression is reprogrammed from somatic cells to iPSCs (Supplementary Fig. 15). FOXO1 had a similar expression pattern to FOXO4 in H9 but not in HUES-6 hESCs (Supplementary Figs 15 and 16). Furthermore, reduction of FOXO4 affected proteasome activity in the multipotent NPCs, which retain partial stem-cell character, but did not affect proteasome activity in differentiated neurons (Supplementary Fig. 18 and Supplementary Table 3). These results raised the question as to whether FOXO4 regulation of proteasome activity could be a general mechanism found in dividing cells. However, we found that FOXO4 was not required for proteasome activity regulation in BJ fibroblasts or HEK293T but rather seems to be specific to hESCs (Supplementary Fig. 19). FOXO4 transcriptional activity is inhibited by phosphorylation on Thr 32, Ser 197 and Ser 262 sites, and once dephosphorylated, it translocates to the nucleus and induces target gene expression[21,22]. Expression of a constitutively active FOXO4 triple alanine mutant (FOXO4-AAA), but not wild-type FOXO4, resulted in further upregulation of proteasome activity in hESCs (Fig. 3c, Supplementary Fig. 20 and Supplementary Table 4a, b). In addition, ectopic expression of FOXO4-AAA in *FOXO4* short hairpin RNA (shRNA) cells partially restored proteasome activity of these cells (Fig. 3d and Supplementary Table 4c). We found that loss of FOXO4 resulted in reduced expression of PSMD11 in hESCs and in the multipotent NPCs, but did not affect PSMD11 in differentiated neurons (Fig. 3e, f and Supplementary Fig. 21). Knockdown of FOXO1, FOXO3 or HSF1 did not affect

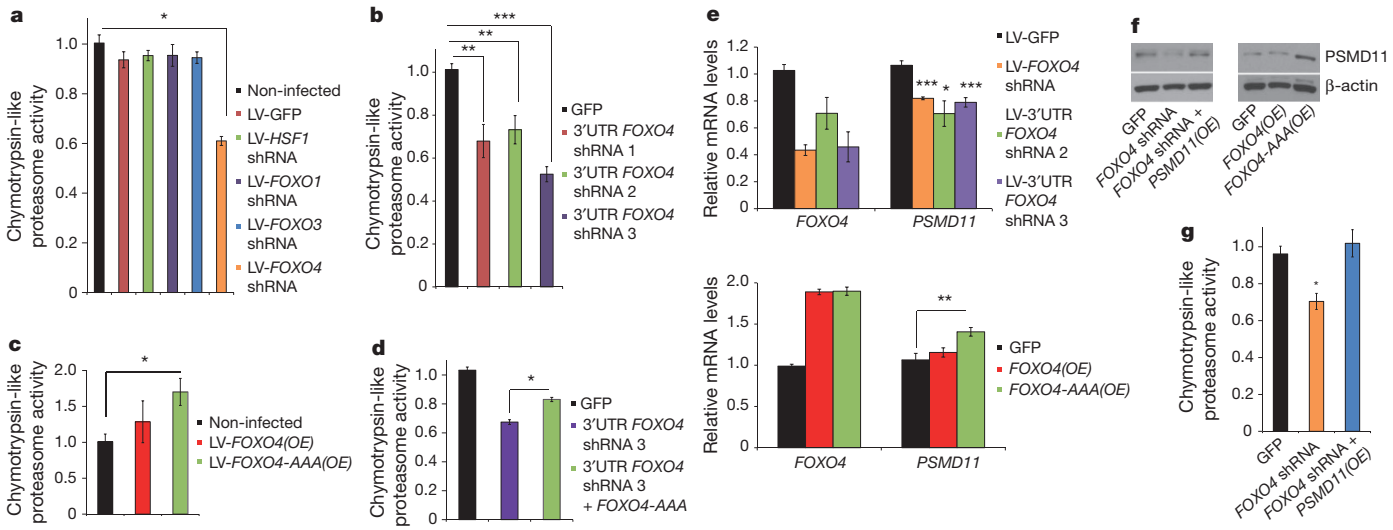

Figure 3 | FOXO4 regulates proteasome activity in hESCs. **a**, Chymotrypsin-like proteasome activity in H9 hESCs transiently infected with lentiviruses (LV; relative slope to non-infected cells) is shown. $n = 19$; $^{*}P < 0.00001$. **b**, Chymotrypsin-like proteasome activity of stable-infected hESCs (relative slope to GFP cells) is shown. GFP ($n = 7$), *FOXO4* shRNA 1 ($n = 6$), *FOXO4* shRNA 2 ($n = 3$), *FOXO4* shRNA 3 ($n = 6$). GFP versus *FOXO4* shRNA 1, $^{**}P < 0.01$; GFP versus *FOXO4* shRNA 2, $^{**}P < 0.01$; GFP versus *FOXO4* shRNA 3, $^{***}P = 4.5 \times 10^{-8}$. All shRNAs target the 3′ untranslated region (UTR) of the human genes. **c**, Proteasome activity of transiently infected hESCs (relative slope to non-infected H9 hESCs) is shown. $n = 7$; non-infected cells versus *FOXO4(OE)* cells, $^{*}P = 0.41$; non-infected cells versus *FOXO4-AAA(OE)* cells, $^{*}P < 0.05$. **d**, Proteasome activity (relative slope to GFP hESCs) is shown. $n = 4$; *FOXO4* shRNA 3 versus *FOXO4* shRNA 3 + FOXO4-AAA, $^{*}P < 0.01$. **e**, Top, knockdown of FOXO4 decreases expression of *PSMD11* in transiently infected H9 hESCs (GFP versus *FOXO4* shRNA, $^{***}P < 0.001$; GFP versus *FOXO4* shRNA 2, $^{*}P < 0.05$; GFP versus *FOXO4* shRNA 3, $^{***}P < 0.001$). GFP ($n = 15$), *FOXO4* shRNA ($n = 19$), *FOXO4* shRNA 2 ($n = 4$), *FOXO4* shRNA 3 ($n = 5$). Bottom, stable overexpression of the FOXO4-AAA mutant increases *PSMD11* expression in H9 hESCs (GFP versus *FOXO4(OE)*, $P = 0.69$; GFP versus *FOXO4-AAA(OE)*, $^{**}P < 0.01$). GFP ($n = 7$), *FOXO4(OE)* ($n = 8$), *FOXO4-AAA(OE)* ($n = 7$). **f**, Western blot analysis of PSMD11 levels. β-actin is the loading control. **g**, Proteasome activity (relative slope to GFP H9 hESCs) is shown. $n = 4$; GFP versus *FOXO4* shRNA, $^{*}P < 0.01$; GFP versus *FOXO4* shRNA + *PSMD11(OE)*, $P = 0.50$. Data in **a**–**e** and **g** represent the mean ± s.e.m. Statistical comparisons were made by Student's *t*-test for unpaired samples.

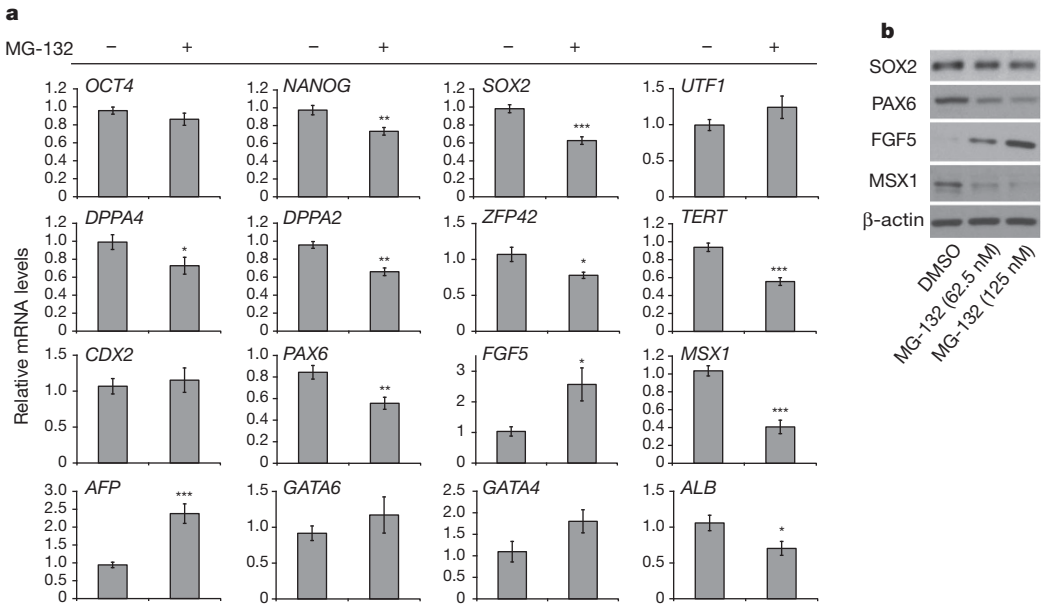

Figure 4 | Acute proteasome inhibition affects pluripotency of hESCs. **a**, Real-time PCR analysis of pluripotency (*OCT4* (also known as *POU5F1*), *NANOG*, *SOX2*, *UTF1*, *DPPA4*, *DPPA2*, *ZFP42* and *TERT*), trophectodermal (*CDX2*), ectodermal (*PAX6*, *FGF5*), mesodermal (*MSX1*) and endodermal (*AFP*, *GATA6*, *GATA4* and *ALB*) germ-layer markers. The graphs (relative expression to H9 hESCs plus dimethylsulphoxide (DMSO)) represent the mean ± s.e.m., $n = 12$. Proteasome inhibition (62.5 nM MG-132 for 24 h) in hESCs induces a decrease in pluripotency markers and modifies the levels of germ-layer markers. *$P < 0.05$; **$P < 0.01$; ***$P < 0.001$. **b**, Western blot analysis with antibodies against SOX2, PAX6, FGF5 and MSX1. β-actin is the loading control. Statistical comparisons were made by Student's *t*-test for unpaired samples.

the expression of PSMD11 in any cell type tested, including hESCs (Supplementary Tables 5–7). Moreover, overexpression of FOXO4-AAA increased PSMD11 levels in hESCs (Fig. 3e, f and Supplementary Table 5). Ectopic expression of PSMD11 in *FOXO4* shRNA hESCs rescued their proteasome activity, indicating that expression of PSMD11 by FOXO4 is sufficient to regulate proteasomal function (Fig. 3f, g).

To test the effects of proteasome inhibition on hESC identity, we induced an acute proteasome inhibition in hESCs by using the MG-132 proteasome inhibitor. Notably, hESCs were more sensitive to proteasome inhibition than were NPCs or neurons, and we had to decrease the MG-132 concentration almost 100 times to avoid cell death and detachment of hESCs (data not shown). Notably, low concentrations of MG-132 (62.5 nM) were sufficient to reduce proteasome activity and induce accumulation of polyubiquitinated proteins in hESCs (Supplementary Fig. 22). Even in the absence of differentiation treatment, we already observed that proteasome inhibition resulted in decreased levels of pluripotency markers and modified the levels of markers of the distinct germ and extraembryonic layers, while decreasing the expression of proteins involved in neurogenesis, such as PAX6 and MSX1 (Fig. 4).

Collectively, our results establish increased proteasome activity as an intrinsic characteristic of hESC identity. Our findings raise the intriguing question of why these cells need enhanced proteasome activity. One possibility is that hESCs cannot tolerate toxic, misfolded proteins, and increased proteostasis could be required to avoid hESC senescence and maintain an intact proteome for either self-renewal or the generation of an intact cell lineage. Alternatively, high proteasome activity may be tightly linked to other cellular process, such as translation, to ensure future integrity of the proteome. In addition, our results indicate that an orthologue of DAF-16, a transcription factor that regulates both lifespan and resistance to proteotoxic stress in invertebrates, crosses evolutionary boundaries and links hESC identity to invertebrate longevity modulation. It will be of particular interest to identify other genes of the proteostasis network regulated by FOXO4 in hESCs. In conclusion, our findings may trigger new advances in understanding hESC differentiation or cell reprogramming and open new possibilities for cell therapy by modulation of the proteostasis network.

METHODS SUMMARY

26S proteasome fluorogenic peptidase assays. The *in vitro* assay of 26S proteasome activities was performed as previously described[10]. Cells were collected in proteasome activity assay buffer (50 mM Tris-HCl, pH 7.5, 250 mM sucrose, 5 mM $MgCl_2$, 0.5 mM EDTA, 2 mM ATP and 1 mM dithiothreitol) and lysed by passing ten times through a 27-gauge needle. Lysate was centrifuged at 10,000*g* for 10 min at 4 °C. Fifteen to twenty-five micrograms of total protein of cell lysates were transferred to a 96-well microtiter plate (BD Falcon) and incubated with fluorogenic substrate. Fluorescence (380 nm excitation, 460 nm emission) was monitored on a microplate fluorometer (Infinite M1000, Tecan) every 5 min for 1 h at 37 °C.

Native gel immunoblotting of the proteasome. HEK293T cells were run on 3.5% native gels prepared in resolving buffer (90 mM Tris base, 90 mM boric acid, 5 mM $MgCl_2$, 0.5 mM EDTA and 1 mM ATP) with 5 mM ATP, 1 mM dithiothreitol and 3.5% acrylamide from a 40% stock solution of acrylamide and bisacrylamide in a 37.5:1 ratio (Bio-Rad). These were run at 110 V for 3 h at 4 °C. Activity assays were performed by incubating the gels in activity assay buffer for 20 min at 37 °C and developed using a BioRad Gel Doc with ultraviolet illumination. Before transfer, the gels were incubated in transfer buffer (25 mM Tris base and 192 mM glycine) with 1% SDS for 10 min followed by a 10-min incubation in transfer buffer. The protein was transferred to polyvinylidene difluoride (PVDF) membranes at 5 V for 16 h in transfer buffer using an Idea Scientific Genie Blotter. Western blot analysis was performed with anti-PSMD1 (Abcam) and analysed using the Odyssey system (LI-COR). Extracts were also analysed by SDS–PAGE to determine protein expression levels and loading control.

A detailed description of all experimental methods, including hESC culture and differentiation, is provided in Methods.

Full Methods and any associated references are available in the online version of the paper.

Received 8 August 2011; accepted 6 August 2012.

1. Evans, M. J. & Kaufman, M. H. Establishment in culture of pluripotential cells from mouse embryos. *Nature* **292,** 154–156 (1981).
2. Thomson, J. A. *et al.* Embryonic stem cell lines derived from human blastocysts. *Science* **282,** 1145–1147 (1998).
3. Isono, E., Saito, N., Kamata, N., Saeki, Y. & Toh, E. A. Functional analysis of Rpn6p, a lid component of the 26 S proteasome, using temperature-sensitive *rpn6*

mutants of the yeast *Saccharomyces cerevisiae*. *J. Biol. Chem.* **280,** 6537–6547 (2005).
4. Pathare, G. R. *et al.* The proteasomal subunit Rpn6 is a molecular clamp holding the core and regulatory subcomplexes together. *Proc. Natl Acad. Sci. USA* **109,** 149–154 (2012).
5. Santamaria, P. G., Finley, D., Ballesta, J. P. & Remacha, M. Rpn6p, a proteasome subunit from *Saccharomyces cerevisiae*, is essential for the assembly and activity of the 26 S proteasome. *J. Biol. Chem.* **278,** 6687–6695 (2003).
6. Kenyon, C., Chang, J., Gensch, E., Rudner, A. & Tabtiang, R. A. C. *elegans* mutant that lives twice as long as wild type. *Nature* **366,** 461–464 (1993).
7. Tatar, M. *et al.* A mutant *Drosophila* insulin receptor homolog that extends life-span and impairs neuroendocrine function. *Science* **292,** 107–110 (2001).
8. Balch, W. E., Morimoto, R. I., Dillin, A. & Kelly, J. W. Adapting proteostasis for disease intervention. *Science* **319,** 916–919 (2008).
9. Powers, E. T., Morimoto, R. I., Dillin, A., Kelly, J. W. & Balch, W. E. Biological and chemical approaches to diseases of proteostasis deficiency. *Annu. Rev. Biochem.* **78,** 959–991 (2009).
10. Kisselev, A. F. & Goldberg, A. L. Monitoring activity and inhibition of 26S proteasomes with fluorogenic peptide substrates. *Methods Enzymol.* **398,** 364–378 (2005).
11. Osafune, K. *et al.* Marked differences in differentiation propensity among human embryonic stem cell lines. *Nature Biotechnol.* **26,** 313–315 (2008).
12. Takahashi, K. *et al.* Induction of pluripotent stem cells from adult human fibroblasts by defined factors. *Cell* **131,** 861–872 (2007).
13. Takahashi, K. & Yamanaka, S. Induction of pluripotent stem cells from mouse embryonic and adult fibroblast cultures by defined factors. *Cell* **126,** 663–676 (2006).
14. Yu, J. *et al.* Induced pluripotent stem cell lines derived from human somatic cells. *Science* **318,** 1917–1920 (2007).
15. Hanna, J. H., Saha, K. & Jaenisch, R. Pluripotency and cellular reprogramming: facts, hypotheses, unresolved issues. *Cell* **143,** 508–525 (2010).
16. Panopoulos, A. D., Ruiz, S. & Izpisua Belmonte, J. C. iPSCs: induced back to controversy. *Cell Stem Cell* **8,** 347–348 (2011).
17. Brennand, K. J. *et al.* Modelling schizophrenia using human induced pluripotent stem cells. *Nature* **473,** 221–225 (2011).
18. Finley, D. Recognition and processing of ubiquitin-protein conjugates by the proteasome. *Annu. Rev. Biochem.* **78,** 477–513 (2009).
19. Köhler, A. *et al.* The axial channel of the proteasome core particle is gated by the Rpt2 ATPase and controls both substrate entry and product release. *Mol. Cell* **7,** 1143–1152 (2001).
20. Coux, O., Tanaka, K. & Goldberg, A. L. Structure and functions of the 20S and 26S proteasomes. *Annu. Rev. Biochem.* **65,** 801–847 (1996).
21. Kops, G. J. P. L. *et al.* Direct control of the Forkhead transcription factor AFX by protein kinase B. *Nature* **398,** 630–634 (1999).
22. Matsuzaki, H., Ichino, A., Hayashi, T., Yamamoto, T. & Kikkawa, U. Regulation of intracellular localization and transcriptional activity of FOXO4 by protein kinase B through phosphorylation at the motif sites conserved among the FOXO family. *J. Biochem.* **138,** 485–491 (2005).

Supplementary Information is available in the online version of the paper.

Acknowledgements We thank W. E. Balch for critical comments on this work. We thank A. Stauffer and V. Modesto for their help with BrdU assays and cell culture, respectively. We thank S. Ruiz for advice on hESC culture and lentiviral infection. This work was supported by the Howard Hughes Medical Institute. D.V. was a recipient of the F.M. Kirby, Inc. Foundation Postdoctoral Scholar Award and Beatriu de Pinós (AGAUR) fellowship. F.H.G. acknowledges the Helmsley Foundation, JPB Foundation, Mathers Foundation, Lookout Fund and California Institute for Regenerative Medicine.

Author Contributions D.V. and A.D. planned and supervised the project. D.V. performed the experiments, data analysis and interpretation. L.B. performed neural differentiation assays and contributed to other assays. I.M. performed biochemistry experiments and contributed to other assays. M.L. performed cell culturing and trophoblast/fibroblast differentiation. C.M. performed biochemistry experiments and contributed to other assays. D.J. performed proteasome assembly experiments. B.S., L.P. and E.M. generated lentiviral constructs. W.T.B. and F.H.G. contributed with their knowledge of stem-cell biology and neural differentiation, and helped to supervise the project. The manuscript was written by D.V. and A.D. and edited by L.B., I.M., C.M., W.T.B. and F.H.G. All authors discussed the results and commented on the manuscript.

Author Information Reprints and permissions information is available at www.nature.com/reprints. The authors declare no competing financial interests. Readers are welcome to comment on the online version of the paper. Correspondence and requests for materials should be addressed to A.D. (dillin@salk.edu).

METHODS

hESCs culture and differentiation. The human H9 (WA09) hESC line was obtained from WiCell Research Institute. The HUES-6 hESC line was obtained from the laboratory of D. Melton. hESC lines were maintained on a mitotically inactive mouse embryonic fibroblast (MEF) feeder layer in hESC medium, DMEM/F12 (Invitrogen) supplemented with 20% knockout serum replacement (Invitrogen), 1 mM L-glutamine, 0.1 mM non-essential amino acids, β-mercaptoethanol and 10 ng ml^{-1} bFGF (Joint Protein Central). When the co-culturing of hESCs with MEFs was not possible owing to interference with downstream assays, H9 hESCs were also maintained on Matrigel (BD Biosciences) using mTeSR1 (Stem Cell Technologies). When cultured on Matrigel, HUES-6 cells were fed conditioned medium collected from cultured MEFs. hESC colonies were passaged using a solution of collagenase (1 mg ml^{-1}) or dispase (2 mg ml^{-1}), and scraping the colonies with a glass pipette. For our experimental assays, we used H9 hESCs passages 40–45 and HUES-6 hESCs passages 30–35. The human iPSC lines (control BJ-iPSC lines) were derived and characterized as previously reported[17] and cultured as described above for hESCs cells.

Neural differentiation was performed as follows. hESCs grown on inactivated MEFs were fed N2/B27 medium (DMEM/F12-GlutaMAX (Invitrogen), N2 (Invitrogen) B27 without retinoic acid (Invitrogen)) for 2 days before being treated with collagenase type IV (1 mg ml^{-1} in DMEM/F12) at 37 °C for 1 h. Once colonies lifted off the plate, they were gently washed and transferred to ultra-low attachment plates (Corning). Aggregates (embryoid bodies) were allowed to form and grown in suspension for 1 week in N2/B27 medium with medium changes as needed, roughly every other day. Embryoid bodies were then transferred onto polyornithine (PORN)/laminin-coated plates in N2/B27 medium with 1 μg ml^{-1} laminin (Invitrogen), where they were allowed to adhere and develop neural rosettes and projections. After 1 week, colonies were picked for NPC lines. Picked colonies containing rosettes or projections are dissociated with TrypLE (Invitrogen) for 5 min at 37 °C and plated onto PORN/laminin coated plates in NPC medium (DMEM/F12, N2/B27-RA (Invitrogen), 1 μg ml^{-1} laminin and 20 ng ml^{-1} FGF2). The resulting monolayer culture was grown at a high density and split 1:3 every week. For our experimental assays, we used NPCs at passages 10–14.

For neuronal differentiation, NPCs were dissociated with TrypLE (Invitrogen) and plated into neuronal differentiation medium (DMEM/F12, N2/B27-RA (Invitrogen), 1 μg ml^{-1} laminin, 20 ng ml^{-1} BDNF (Peprotech), 20 ng ml^{-1} GDNF (Peprotech), 1 mM dibutyryl-cyclic AMP (Sigma) and 200 nM ascorbic acid (Sigma)) onto PORN/laminin-coated plates. For this study, cells were differentiated in 6-well plates, with approximately 2×10^5 cells per well. Cells were differentiated for 2–3 months, with weekly feeding of neuronal differentiation medium.

Differentiation to fibroblast cells involved the formation of embryoid bodies as described above, but cultured in embryoid body medium (IMDM base medium supplemented with 15% FBS (Atlanta Biologicals), 0.1 mM non-essential amino acids and 1% glutamax (Invitrogen)) and maintained on ultra-low attachment plates with daily medium changes. One week later the floating embryoid bodies were plated on gelatin-coated plates and passaged at confluence three times before use. Alternatively, a non-embryoid body method was used involving the individualization of hESCs using Accutase (Millipore) and plating the cells at a density of 2.5×10^4 cells per cm^2 in embryoid body medium containing ROCK inhibitor (Stemgent) at 10 μM. The cells were fed daily with straight embryoid body medium. At confluence, any areas still showing a stem-cell-like morphology were removed by aspiration and then passaged using Accutase. After three passages, the cells present had fibroblast morphology and were confirmed by PCR of lineage-specific markers.

Trophoblast differentiation was performed as described previously using high levels of BMP4 (ref. 23). Keratinocyte differentiation was performed following the protocol established in ref. 24. BJ human fibroblasts (ATCC) were cultured in DMEM (Invitrogen) supplemented with 10% FBS and 0.1 mM non-essential amino acids, and passaged with trypsin. Hippocampal and cerebellar astrocytes are from Sciencell.

Generation of lentiviral vectors. The shRNA-expressing lentiviral vectors were generated by cloning the sequences described in Supplementary Table 8 into the pSIH1-copGFP vector (SBI Biosystems) to generate pLV-siHSF-1, pLV-siFOXO1, pLV-siFOXO3, pLV-siFOXO4, pLV-si3′UTR_1 FOXO4, pLV-si3′UTR_2 FOXO4 and pLV-si3′UTR_3 FOXO4. A control shRNA vector was generated by cloning the sequence 5′-CGTGCGTTGTTAGTACTAATCCTATTT-3′ designed against the sequence of luciferase (SBI Biosystems) into the same vector to generate pLV-siLuc. The GFP-expressing vector was prepared from the third generation self-inactivating lentivirus[25]. Lentiviruses were packaged by transient transfection in 293T cells[25].

Lentivirus (LV)-non targeting shRNA control, LV-shPSMD11_1 (clone number TRCN0000003948), LV-shPSMD11_2 (TRCN0000003950), LV-shPSMC2_1(TRCN0000007181), LV-shPSMC2_2 (TRCN0000007183) in pLKO.1-puro-CMV-tGFP vector were obtained from Mission shRNA (Sigma). FOXO4-overexpressing lentiviral constructs (*FOXO4(OE)*) were generated as follows. Flag–FOXO4 construct was obtained from Addgene (plasmid 17549). PCR was performed to generate a product to be cloned into pLVX puro lentiviral plasmid (Clontech) using the XhoI/SmaI sites. Forward primer (with 5′ XhoI site for cloning): 5′-CGCGTACTCGAGATGGATCCGGGGAATGAGAATTCAGC CACAGAGGCTGCCGCGATCATAGAC-3′; reverse primer (with 3′ SmaI site for cloning): 5′-CCGGAACCCGGGTCAGGGATCTGGCTCAAAG-3′. To generate FOXO4-AAA (Thr 32, Ser 197, Ser 262), site-directed mutagenesis of wild-type FOXO4 was performed by using Pfu Turbo. The primers used for site-directed mutagenesis were: Thr32Ala, forward, 5′-GTCCCCGCTCCT GTGCTTGGCCCCTTCC-3′; reverse, 5′-GGAAGGGGCCAAGCACAGGAG CGGGGAC-3′. Ser197Ala, forward, 5′-GCAAAGCCCCCCGCCGCAGAGCC GCAGCCATGGATAGCAGCAG-3′; reverse, 5′-CTGCTGCTATCCATGGCT GCGGCTCTGCGGCGGGGGGCTTTGC-3′. Ser262Ala, forward, 5′-GTCCAC GAAGCAGCGCAAATGCCAGCAGTGTCAGC-3′; reverse, 5′-GCTGACACT GCTGGCATTTGCGCTGCTTCGTGGAC-3′.

PCR was performed with one set of primers at a time. DpnI was added to the PCR product for 2 h at 37 °C before transformation of DH5a bacteria. Plasmid preps were sequenced before the next mutation introduced.

PSMD11-overexpressing lentiviral construct (*PMSD11(OE)*) was generated as follows. Human *PSMD11* complementary DNA was PCR-amplified and cloned into pLVX-Puro using XhoI and BamHI. Resulting constructs were transformed into One Shot Stbl3 *Escherichia coli* (Invitrogen). Constructs were sequence verified and thereafter transfected into packaging cells to produce high titre lentiviruses.

Lentiviral infection of human stem cells. hESC colonies growing on Matrigel were incubated with mTesR1 medium containing 10 μM ROCK inhibitor for 1 h and individualized using Accutase. Fifty-thousand cells were infected in suspension with 10 μl of concentrated lentivirus in the presence of 10 μM ROCK inhibitor. Cell suspension was centrifuged to remove virus, passed through a mesh of 40 μM to obtain individual cells, and plated back on a feeder layer of fresh MEFs in hESC media supplemented with 10 μM ROCK inhibitor. After a few days in culture, small hESC colonies arose. For the GFP and *FOXO* shRNA lentiviral stable lines, GFP-positive colonies were selected and manually passaged onto fresh MEFs to establish new hESC lines. For non-targeting shRNA lentivirus, *PSMD11* shRNA, *PSMC2* shRNA, *FOXO4(OE)* shRNA, *FOXO4-AAA(OE)* shRNA and *PSMD11(OE)* shRNA stable lines, we performed 1 μg ml^{-1} puromycin-resistance selection during three days and then colonies were manually passaged onto fresh MEFs to establish new hESC lines.

Transient infection experiments were performed as follows. hESC colonies growing on Matrigel were incubated with mTesR1 medium containing 10 μM ROCK inhibitor for 1 h and individualized using Accutase. Ten thousand cells were plated on Matrigel plates and incubated with mTesR1 medium containing 10 μM ROCK inhibitor for 1 day. Cells were infected with 2 μl of concentrated lentivirus. Plates were centrifuged at 800*g* for 1 h at 30 °C. Cells were fed with fresh media the day after to remove virus. NPCs were split as described above, and infected with 2 μl of concentrated lentivirus for 1 day. Neurons were infected after 2 months of differentiation with 2 μl of concentrated lentivirus for 1 day. In all the cases, cells were collected for experimental assays after four days of infection.

26S proteasome fluorogenic peptidase assays. The *in vitro* assay of 26S proteasome activities was performed as previously described[10]. Cells were collected in proteasome activity assay buffer (50 mM Tris-HCl, pH 7.5, 250 mM sucrose, 5 mM $MgCl_2$, 0.5 mM EDTA, 2 mM ATP and 1 mM dithiothreitol) and lysed by passing ten times through a 27-gauge needle attached to a 1-ml syringe. Lysate was centrifuged at 10,000*g* for 10 min at 4 °C. Approximately 15–25 μg of total protein of cell lysates were transferred to a 96-well microtiter plate (BD Falcon), and the fluorogenic substrate was then added to lysates. To measure the chymotrypsin-like activity of the proteasome we used either Z-Gly-Gly-Leu-AMC (Enzo) or Suc-Leu-Leu-Val-Tyr-AMC (Enzo). We used Z-Leu-Leu-Glu-AMC (Enzo) to measure the caspase-like activity of the proteasome, and Ac-Arg-Leu-Arg-AMC for the proteasome trypsin-like activity. Fluorescence (380 nm excitation, 460 nm emission) was monitored on a microplate fluorometer (Infinite M1000, Tecan) every 5 min for 1 h at 37 °C. Protein concentration of the cell homogenates was determined using the BCA protein assay (Pierce). For SDS experiments, 0.025% SDS was added to cell lysates 5 min before the digestion assay.

Native gel immunoblotting of the proteasome. hESCs (H9), NPCs and neurons were collected in proteasome activity assay buffer (50 mM Tris-HCl, pH 7.6, 5 mM $MgCl_2$, 0.5 mM EDTA, 5 mM ATP, 1 mM dithiothreitol and 10% glycerol supplemented with Roche phosphatase inhibitors) and lysed by passing ten times

through a 27-gauge needle attached to a 1-ml syringe. Lysate was centrifuged at 16,000*g* for 15 min at 4 °C. Fifteen micrograms of total protein was run on a 3–12% NativePAGE Bis-Tris gel (Invitrogen) in NativePAGE running buffer (Invitrogen) at 4 °C for 1 h at 150 V and then increased to 200 V for a further hour. Proteins were then transferred to a polyvinylidene difluoride (PVDF) membrane at 25 V for 1 h in NativePAGE transfer buffer (Invitrogen) in an XCell II Blot module (Invitrogen). After transfer, the PVDF membrane was incubated for 20 min with 8% acetic acid to fix the proteins and then dried. Western blot analysis was performed with anti-20S alpha 1–7 (Abcam) and anti-PSMD2 (Abcam).

HEK293T cells were run on 3.5% native gels prepared in resolving buffer (90 mM Tris base, 90 mM boric acid, 5 mM $MgCl_2$, 0.5 mM EDTA and 1 mM ATP) with 5 mM ATP, 1 mM dithiothreitol and 3.5% acrylamide from a 40% stock solution of acrylamide and bisacrylamide in a 37.5:1 ratio (Bio-Rad). These were run at 110 V for 3 h at 4 °C. Activity assays were performed by incubating the gels in activity assay buffer for 20 min at 37 °C and developed using a BioRad Gel Doc with ultraviolet illumination. Before transfer, the gels were incubated in transfer buffer (25 mM Tris base and 192 mM glycine) with 1% SDS for 10 min followed by a 10-min incubation in transfer buffer. The protein was transferred to PVDF membranes at 5 V for 16 h in transfer buffer using an Idea Scientific Genie Blotter. Western blot analysis was performed with anti-PSMD1 (Abcam) and analysed using the Odyssey system (LI-COR Biosciences). Extracts were also analysed by SDS–PAGE to determine protein expression levels and loading control.

Western blot. For analysis of proteasome subunits, cells were collected in proteasome activity assay buffer supplemented with protease inhibitors (Roche) and lysed by passing ten times through a 27-gauge needle attached to a 1-ml syringe. Lysate was centrifuged at 10,000*g* for 10 min at 4 °C. Protein concentration of the cell homogenates was determined using the BCA protein assay (Pierce). For analysis of transcription factor and polyubiquitinated proteins, cells were collected from tissue culture plates by cell scraping and lysed in protein cell lysis buffer (10 mM Tris-HCl, pH 7.4, 10 mM EDTA, 50 mM NaCl, 50 mM NaF, 1% Triton X-100, 0.1% SDS supplemented with 2 mM sodium orthovanadate, 1 mM phenylmethylsulphonyl fluoride and Complete mini protease and PhosSTOP inhibitor cocktail mix) for 2 h at 1,000 r.p.m. and 4 °C in a Thermomixer. Protein concentrations were determined with a standard Bradford protein assay (BioRad). Approximately 20–50 μg of total protein was separated by SDS–PAGE, transferred to nitrocellulose membranes (Whatman) and subjected to immunoblotting. Western blot analysis was performed with anti-FK1 (Enzo), anti-20S alpha 1–7 (Abcam), anti-proteasome 20S C2 (Abcam), anti-Rpt6 (Biomol), anti-PSMD1 (Abcam), anti-PSMD2 (Abcam), anti-PSMD14 (Abcam), anti-PSMB6 (Abcam), anti-PSMD11 (Novus), anti-FOXO4 (55D4) (Cell Signaling), anti-FOXO1 (C29H4) (Cell Signaling), anti-SOX2 (D6D9) (Cell Signaling), anti-FGF5 (Abcam), anti-MSX1 (Abcam), anti-PAX6 (Abcam) and anti-β-actin (Abcam). The affinity of the antibody to PSMD11 has been characterized by detecting a decrease at the protein levels with *PSMD11* shRNA or an increase by ectopic expression of PSMD11. These experiments convincingly show differences in only one band and we ascribe any alteration of PSMD11 to this band.

Coomassie staining. Protein lysates were separated by SDS–PAGE and visualized directly in the gel by Coomassie staining[26]. Gels were incubated in fixing solution (50% methanol, 10% acetic acid and 100 mM ammonium acetate) for 60 min, stained with 0.025% Coomassie dye in 10% acetic acid on a shaker overnight and destained twice in 10% acetic acid for 60 min. Gels were transferred to water and analysed with the Odyssey imager (Li-Cor Bioscience).

Bromodeoxyuridine proliferation assay. Cells were incubated with media containing 10 mM bromodeoxyuridine (BrdU) for 40 min. Cells were fixed with formaldehyde 4% in PBS for 15 min and washed in PBS. Before permeabilization, cells were incubated for 1 h in 2 N HCl at room temperature followed by extensive washes in PBS. Cells were permeabilized with 0.5% Triton X-100 in PBS for 10 min and blocked with 5% normal donkey serum in 1% PBS-BSA for 40 min at room temperature. Rabbit anti-BrdU antibody (ABD Serotech) was diluted in 1% PBS-BSA and used for overnight incubation followed by incubation with a biotinylated anti-rabbit secondary antibody (Vector) for a further 2 h at room temperature. Finally, cells were incubated with streptavidin-AlexaFluor 568 (Jackson Immuno Research) for 1 h. DAPI was used to visualize nuclei at a concentration of 0.5 μg ml^{-1} in PBS.

RNA isolation and quantitative RT–PCR. Total RNA was extracted using RNAbee (Tel-Test Inc.). cDNA was created using the Quantitect reverse transcriptase kit (Qiagen). SybrGreen real-time qPCR experiments were performed as described in the manual using ABI Prism79000HT (Applied Biosystems) and cDNA at a 1:20 dilution. Data was analysed with the comparative $2\Delta\Delta C_t$ method using β-actin and *GAPDH* as housekeeping genes. See Supplementary Table 9 for details about the primers used for this assay.

23. Xu, R. H. *et al.* BMP4 initiates human embryonic stem cell differentiation to trophoblast. *Nature Biotechnol.* **20,** 1261–1264 (2002).
24. Itoh, M., Kiuru, M., Cairo, M. S. & Christiano, A. M. Generation of keratinocytes from normal and recessive dystrophic epidermolysis bullosa-induced pluripotent stem cells. *Proc. Natl Acad. Sci. USA* **108,** 8797–8802 (2011).
25. Tiscornia, G., Singer, O. & Verma, I. M. Design and cloning of lentiviral vectors expressing small interfering RNAs. *Nature Protocols* **1,** 234–240 (2006).
26. Schägger, H. Tricine–SDS-PAGE. *Nature Protocols* **1,** 16–22 (2006).